7th International Symposium on High-Temperature Metallurgical Processing
Edited by: Jiann-Yang Hwang, Tao Jiang, P. Chris Pistorius, Gerardo R.F. Alvear F., Onuralp Yücel, Liyuan Cai, Baojun Zhao, Dean Gregurek, and Varadarajan Seshadri
TMS (The Minerals, Metals & Materials Society), 2016

KINETICS STUDY ON THE PYROLYSIS OF LOW GRADE COALS

Ruiling DU, Keng WU*, Xiao YUAN, Daan XU, Changyao CHAO

State Key Laboratory of Advanced Metallurgy, University of Science and Technology Beijing
Beijing 100083, China
Email: 541348637@qq.com
Keywords: Kinetics, pyrolysis, coal, semi-coke

Abstract

To utilize low grade coals to produce high quality semi-coke which can be used in blast furnaces, the pyrolysis of low grade coals was studied in this paper. According to the characteristics of coal pyrolysis process, the temperature range was divided into three parts. The interfacial chemical reaction model, random pore model and the internal diffusion model with the shrinking volume of resultant were established to describe the different ranges of pyrolysis process respectively. The results showed that the experimental data was fitted well, and all the correlation coefficients (r^2) exceeded 0.97. Finally, the kinetic parameters for each temperature range have been calculated, which laid a necessary foundation for the simulation and expanded production.

Introduction

With the utilization of coals resources, high grade coals reserve is reducing sharply. Due to less carbon content, high volatile and other characteristics, low grade coals can't be directly used into blast furnaces. They should be transformed to semi-coke by retorting. The semi-coke could be widely used in iron making [1, 2].1) The semi-coke replaced part of anthracite can be injected into blast furnaces. 2) A small number of semi-cokes mixed with sinter could be added into blast furnaces. Because the reactivity of semi-coke with CO_2 is higher than coke, the consumption of coke can be reduced. 3) Semi-cokes are often used to produce ferronickel in the process of RKEF. In order to produce high quality semi-coke, the pyrolysis kinetics of coal should be further studied, which can lay a solid foundation for the process of producing semi-coke. In addition, the pyrolysis process of coals, which has obvious effects on the ignition and combustion, is an important part of coals gasification [3]. Therefore, further study on the pyrolysis process of coals can help us utilize the resources effectively [4].

According to the characteristics of pyrolysis process, the temperature range could be divided into three parts [5, 6]. First, the adsorbed gas and crystal water were removed. With a large amount of coal gas and tar vapors evaporating off, coal was transformed into semi-coke in the second phase. In the third range, the semi-coke was further coked. The reaction mechanisms were different in the diverse temperature ranges. It was unreasonable that the whole pyrolysis process was fitted with a single model [7]. Therefore, the interfacial chemical reaction model, random pore model and the internal diffusion model with the shrinking volume of resultant were established respectively to study the pyrolysis kinetics of coals. Finally, the kinetic parameters of each stage are calculated, which can be widely used in the simulation and expanded production. Meanwhile, the mechanisms and rate-controlling links can be obtained, which can be used to predict the reaction rate and degree of difficulty.

Kinetics Models

Interfacial chemical reaction model

The adsorbed gas and crystal water were removed in the low-temperature range. Gaseous product easily overflowed from the solid product. Therefore, interface chemical reaction model was used to the first phase. Assumptions: the reaction particles A is a compact sphere; the reaction type is interface chemical reaction; the chemical reaction equation is A (s) =aG (g) +bS (s) [8].

When the stage of interfacial chemical reaction is the rate-controlling link, the consumption rate of sample A is equal to the interfacial chemical reaction rate, namely $\upsilon_A = -\frac{4\pi r^2 \rho_A}{M_A}\frac{dr}{dt} = \upsilon_C = 4\pi r^2 k_{rea}$. The integral equation can be described as follows:

$$\int_{t_0}^{t_1} \delta_1 k_{rea}\, dt = y_1(\alpha) \tag{1}$$

Where, $\delta_1=M_A/\rho_A R_0$; $y_1(\alpha)=1-(1-\alpha)^{1/3}$; The conversion rate α is $\alpha = (R_0^3 - r^3)/R_0^3$; M_A is the relative molecular mass of sample A; ρ_A is the density of sample A, $g \cdot m^{-3}$; r refers to the reactant A radius, m; R_0 refers to the initial radius of sample A, m.

The function $dT=\beta dt$ and the equation $k_{real} = A_1 e^{-\frac{E_{a1}}{RT}}$ are inserted into Eq. (1). The Eq. (2) can be obtained.

$$\ln\frac{y_1(\alpha)}{T^2} = \ln\frac{\delta_1 A_1 R}{\beta E_{a1}} - \frac{E_{a1}}{RT} \tag{2}$$

Where, k_{real} is the constant of interface chemical reaction rate, $m \cdot s^{-1}$; A_1 is the former factor, $m \cdot s^{-1}$; E_{a1} is the reaction activation energy, $J \cdot mol^{-1}$.

According to the linear relationship of $\ln[y_1(\alpha)/T^2]$ and $1/T$ in equation (2), the slope and intercept of the curve can be obtained in terms of the fitting results in the low-temperature range. And then, E_{a1}, A_1, and the function of k_{real} and T can be calculated.

Random pore model

Coals were transformed into semi-coke in the middle-temperature range. The reaction rate was related to the specific surface area, which was enlarged with a large number of pores emerging. The random pore model was adopted to describe the process. Assumptions: the microporous consisted of cylindrical hole with arbitrary radius are randomly distributed in the solid reactants; pyrolysis reaction mainly occurs on the surface of micropores; in terms of ignoring the effect of diffusion, the pyrolysis rate of coal is equal to the chemical reaction rate, which has a proportional relation with the specific surface area [9, 10].

By introducing the pore structure parameters, the random pore model is successfully applied to gas-solid reaction process which has a low conversion rate (0~0.6) and exists a maximum reaction rate or gradually reduced. The relationship for fitting can be expressed as follows:

$$\ln\frac{y_2(\alpha)}{T^2} = \ln\frac{\delta_2 \psi A_2 R}{\beta E_{a2}} - \frac{E_{a2}}{RT} \tag{3}$$

Where, $y_2(\alpha)=\sqrt{1-\psi\ln(1-\alpha)}$; $\psi=\frac{4\pi L_0(1-\varepsilon_0)}{S_0^2}$; $\delta_2=\frac{3(1-\varepsilon_0)M_A}{2\rho_A R_0 S_0}$; S_0, is the initial surface area; L_0 is the total length of the initial pore; ε_0 is the initial void ratio.

Similarly, according to the relationship of $\ln[y_2(\alpha)/T^2]$ and $1/T$ in Eq.(3), the experimental data of pyrolysis at the middle-temperature range can be fitted. Finally, E_{a2}, A_2, and the fuction of k_{rea2} and T can be obtained.

Internal diffusion model with the shrinking volume of resultant

In the third range, the semi-coke was further coked with the obvious volume shrinkage. With the high temperature, the chemical reaction rate was higher than the diffusion. The internal diffusion model with the shrinking volume of resultant is adopted [11]. When the stage of gas internal diffusion is the rate-controlling link, the consumption rate of sample A is equal to gas diffusion rate. It meets the relation $\upsilon_D=a\upsilon_A$, namely $-\frac{4\pi r^2 a\rho_A}{M_A}\frac{dr}{dt}=4\pi r^2 D\frac{dc}{dr}$. The equation can be expressed as follows:

$$\ln\frac{y_3(\alpha)}{T^2}=\ln\frac{\delta_3 D_0 R}{\beta E_{a3}}-\frac{E_{a3}}{RT} \tag{4}$$

Where, $\delta_3=\frac{6M_A(c_i-c_0)}{a\rho_A R_0^2}$; $y_3(\alpha)=(1+V\alpha-\alpha)^{2/3}\left[1-3\left(\frac{1-\alpha}{1+V\alpha-\alpha}\right)^{2/3}+2\left(\frac{1-\alpha}{1+V\alpha-\alpha}\right)\right]$; $D=D_0e^{-\frac{E_{a3}}{RT}}$; V is the volume ratio of solid resultants and reactants, $V=(R_x^3-r^3)/(R_0^3-r^3)$; c_i and c_0 are the gas concentration of internal and external surface the solid material respectively, $mol\cdot m^{-3}$; D is the effective diffusion coefficient, $m^2\cdot s^{-1}$; D_0 is frequency factor, $m^2\cdot s^{-1}$; a is the stoichiometric number of the gas resultants; R_x is the radius of simple A at temperature T, m.

Similarly, E_{a3} and D_0 can be acquired in terms of the relationship between $\ln[y_3(\alpha)/T^2]$ and $1/T$.

Materials and Methods

Low grade coal A was taken into the experiment. It belongs to bituminous coal and has characteristics of high volatilization. The proximate and ultimate analysis of Coal A was shown in table 1.

Table 1. Proximate and ultimate analysis of Coal A (%)

Proximate analysis				Ultimate analysis				
F_{Cd}	A_d	V_d	M_{ad}	C	H	N	S	O
53.30	8.57	31.21	6.92	65.53	6.05	1.06	0.43	8.44

The comprehensive thermogravimetric analyzer made in Germany Netzsch No. STA 409 C was adapted to the experiment. The sample was heated automatically according to the setting program. And the experimental data was collected automatically by the computer.

The size of sample was prepared to 0.074 ~0.147 mm. The mass of sample was 10~15 mg in each experiment. During the experimental process, the sample was placed at room temperature for 40 minutes to exhaust the air, heated to 105 ℃ at the rate of 10 K/min staying for 10 minutes to remove the adsorbed water, and heated to 900℃ at the different heating rates (5, 25, and 45 K/min). In the experimental process, the gas flow 150 mL/min of high purity nitrogen ($N_2\geq$ 99.999%) was adopted to protect the sample from oxidation.

Results

Coal is a kind of heterogeneous polymer compounds. The main decomposed products of coal are combustible gas, tar, and semi-coke. The mass loss and derivative mass loss curves of pyrolysis process at different heating rates were shown in Fig. 1 and 2.

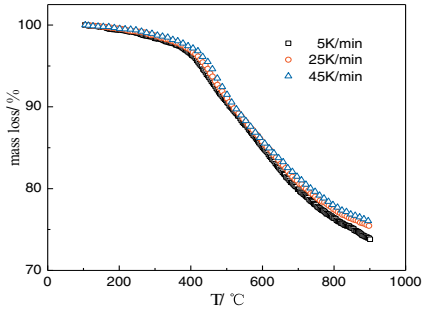

Fig. 1. TG curves of pyrolysis process at different heating rates

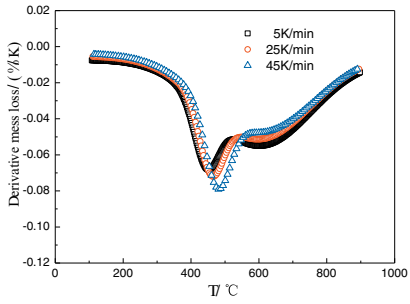

Fig. 2. DTG curves of pyrolysis process at different heating rates

According to the characteristics of curve, the pyrolysis process could be divided into three parts. First, the adsorbed gas and crystal water were removed in the low-temperature range. Meanwhile, the weak keys of coal decomposed. In this part, the heating rates had a little effect on the weight loss rates which maintained at a low level. The pyrolysis rate increased sharply at around 386 °C, which indicated the reaction mechanism and the rate-controlling link were changing.

Second, the reactions occurred in the middle-temperature range were mainly dominated by the depolymerization and decomposition reaction with a large amount of coal gas, tar vapors and etc evaporating off. With the temperature rising, the coal was transformed into semi-coke. Meanwhile, with the heating rate rising, the weight loss of coal A decreased, and the degree of pyrolysis showed a decline. The pyrolysis reaction rate reached maximum at about 470 °C. With the heating rate rising, the maximum increased, and the temperature corresponding to the peak shifted to the high temperature region.

Third, the reactions taken place in the high-temperature range was mainly dominated by Polycondensation reaction with little tar and volatile. Meanwhile, the semi-coke was further coked with the obvious volume shrinkage. At the same temperature, the faster the heating rate raised the more slowly the rate of coal a pyrolyzed. The effect of the heating rates on pyrolysis rates decreased with increasing temperature [12, 13].

Discussion

Temperature range division

According to the characteristics of pyrolysis process, the temperature range could be divided into three parts at the temperature where the variation of weight loss rate reached the maximum. The divided ranges were showed in table 2.

Table 2. Temperature ranges at different heating rates

Heating rates β (K/min)	Low-temperature range /(℃)	Middle-temperature range /(℃)	High-temperature range /(℃)
5	105~369	369~497	497~900
25	105~386	386~524	524~900
45	105~399	399~548	548~900

Based on the table 2, the temperature ranges were various at different heating rates due to the effects of heating rates in the pyrolysis process. The sectioning temperature points were higher as the heating rates enhanced.

Fitting results

According to the table 2, the experimental data of different temperature ranges at various heating rates could be fitted by Eq.(2), Eq.(3), and Eq.(4) respectively. The results were showed in Fig.3, Fig.4, Fig.5, and table 3. In the figures, "□、○、△" respectively represented experimental data at different heating rates, and the lines represented the fitting results of models.

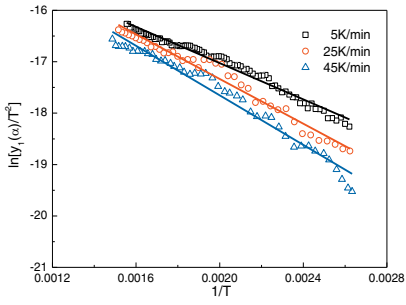

Fig. 3. Fitting Curves in low-temperature range

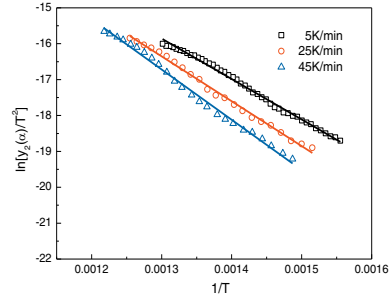

Fig. 4. Fitting Curves in middle-temperature range

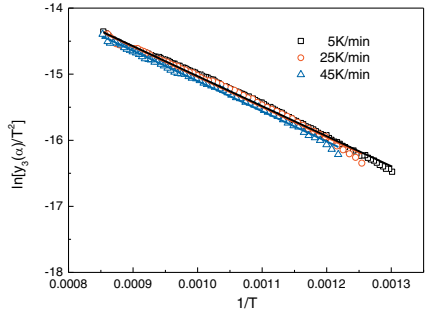

Fig. 5. Fitting Curves in high-temperature range

Table 3. Correlation coefficients (r^2) in three ranges under different heating rates

Heating rates(K/min)	r_1^2	r_2^2	r_3^2
5	0.9724	0.9928	0.9935
25	0.9716	0.9952	0.9959
45	0.9783	0.9949	0.9960

According to Fig.3, Fig.4, Fig.5, and table 3, the experimental data was fitted well, and all the correlation coefficients (r^2) exceeded 0.97. The interface chemical reaction model, random pore model and internal diffusion model with the shrinking volume of resultant were suitable to describe the three ranges of pyrolysis process respectively.

Corresponding kinetic parameters

Based on the slopes and intercepts of fitted curve and relevant parameters, the kinetic parameters in three ranges at different heating rates could be calculated. The results were listed in tables 4, 5, and 6. Where, R_0=1.11×10^{-4} m; ρ_A=1.28×10^6 g/m^3; c_i=1 mol/m^3; M_A=131; ψ=1; c_0=0 mol/m^3; a=1; V=0.733.

Table 4. Corresponding Kinetic Parameters in the low-temperature range

Heating rate β (K/min)	Temperature range T (℃)	Activation energy E_{a1} (J/mol)	Former factor A_1 (m·s^{-1})	Chemical reaction rate constant k_{rea1} (m·s^{-1})
5	105~369	1.47×10^4	2.19×10^{-4}	lnk_{rea1}=-1.76×10^3/T-8.43
25	105~386	1.81×10^4	2.61×10^{-3}	lnk_{rea1}=-2.17×10^3/T-5.95
45	105~399	2.00×10^4	4.49×10^{-3}	lnk_{rea1}=-2.41×10^3/T-5.41

Table 5. Corresponding kinetic parameters in the middle-temperature range

Heating rates β (K/min)	Temperature range T (℃)	Activation energy E_{a2} (J/mol)	Former factor A_2 (m·s^{-1})	Chemical reaction rate constant k_{rea2} (m·s^{-1})
5	369~497	5.58×10^4	7.28×10^{-3}	lnk_{rea2}=-6.71×10^3/T-4.92
25	386~524	6.04×10^4	9.45×10^{-2}	lnk_{rea2}=-7.26×10^3/T-2.36
45	399~548	6.67×10^4	5.37×10^{-1}	lnk_{rea2}=-8.02×10^3/T-0.62

Table 6. Corresponding kinetic parameters in the high-temperature range

Heating rates β (K/min)	Temperature range T (℃)	Diffusion activation energy E_{a3} (J/mol)	Frequency factor D_0 (m^2·s^{-1})	Effective diffusion coefficient D (m^2·s^{-1})
5	497~900	3.78×10^4	2.12×10^{-7}	lnD=-4.54×10^3/T-15.37
25	524~900	3.80×10^4	4.31×10^{-7}	lnD=-4.57×10^3/T-14.66
45	548~900	3.81×10^4	8.23×10^{-7}	lnD=-4.58×10^3/T-14.01

In the tables 4, 5, and 6, the activation energy at the same rate-controlling link increased with the heating rates, but the magnitude of variation was less. The minimum activation energy ranged from 14kJ/mol to

20kJ/mol existed in the low-temperature range. Adsorbed gas and crystal water were removed in this process, which need less power. The maximum activation energy (55~ 67kJ/mol) existed in the second range. The main reactions were macromolecule dissociation of coal and further decomposition of macromolecules in split product, which need more power. The activation energy with minimum variation scope ranged from 37kJ/mol to 39kJ/mol existed in high-temperature range. The semi-coke coked further in this process.

Furthermore, according to the functions of chemical reaction rate constant and effective diffusion coefficient with temperature listed in the tables 4, 5, and 6**,** the kinetic parameters at different temperatures could be calculated. The results were shown in Fig. 6.

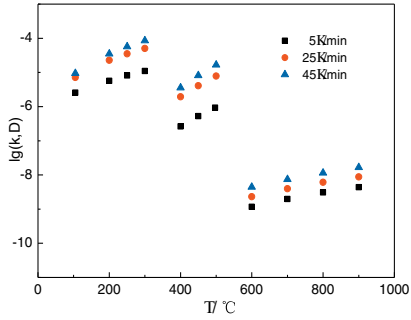

Fig. 6. Corresponding kinetic parameters (in logs) at different temperature

Magnitudes of reaction rate constant felled into 10^{-7}~10^{-5}. Magnitudes of effective diffusion coefficient ranged from 10^{-10} to 10^{-8}. The magnitudes of reaction rate constant had exceeded effective diffusion coefficient about 2~3 magnitudes, which conformed well to data scholars at home and abroad had measured [14, 15].The chemical reaction rate constant or effective diffusion coefficient increased with heating rates at the same temperature, and also increased with the temperature.

Conclusion

According to the characteristics of pyrolysis process, the temperature range was divided into three parts at the temperature where the variation of weight loss rate reached the maximum. The adsorbed gas and crystal water were removed in the low-temperature range. With a large amount of coal gas and tar vapors evaporating off, coal was transformed into semi-coke in the second phase. In the third range, the semi-coke was further coked.

The reaction mechanisms were different in the diverse temperature ranges. The interfacial chemical reaction model, random pore model, and the internal diffusion model with the shrinking volume of resultant were successfully applied to the pyrolysis process of coal. Finally, the functions of reaction rate constants and effective diffusion coefficient with temperature were obtained, which could provide necessary parameters for the utilization coal resource.

With the heating rate increasing, the whole pyrolysis process of coal revealed a thermal hysteresis phenomenon. The activation energy at the same rate-controlling link increased with the heating rates. The chemical reaction rate constant or effective diffusion coefficient increased with the heating rates at the same temperature, and also increased with the temperature.

Acknowledgements

The authors are grateful for support from the National Science Foundation China (Grant No. 51274026), the Independent Research Project of State Key Laboratory of Advanced Metallurgy (Grant No. 41603003), University of Science and Technology Beijing (USTB), China. Correspondence author: Keng WU, E-mail: 541348637@QQ.com.

References

1. Q. H. Liu, K. Wu, and H. Y. Wang, "Kinetic study of tar's separation from coals used in COREX," *Journal of China Coal society*, 37(10) (2012), 1749-1752.
2. Y. B. Zhang, G H. Li, and T. Jiang, "Reduction behavior of tin-bearing iron concentrate psellets using diverse coals as reducers," *International Journal of Mineral Processing,* 110 (2012), 109–116.
3. J. Tomeczek and H. Plaugniok, "Kinetics of mineral matter transformation during coal combustion," *Fuel*, 81 (2002), 1251-1258.
4. S. F. Zhang, F. Zhu, and C. G Bai, "High temperature pyrolysis behaviour and kinetics of lump coal in COREX melter gasifier," *Ironmaking and steelmaking*, 41(3) (2014), 219-228.
5. A. O. Aboyade, J. F. Görgens and M. Carrier, "Thermogravimetric study of the pyrolysis characteristics and kinetics of coal blends with corn and sugarcane residues," *Fuel processing Technology*, 106 (2013), 310–320.
6. H. M. Jeong, M. W. Seo, and S. M. Jeong, "Pyrolysis kinetics of coking coal mixed with biomass under non-isothermal and isothermal conditions," *Bioresource Technology*, 155 (2014), 442– 445.
7. K. Wu, Q. H. Liu, and W. L. Zhan, "Research on Tar Precipitation Kinetics Using Phasewise Analysis," *Journal of Chemical Engineering of Chinese Universities*, 28(4) (2014), 738-744.
8. H. J. Guo, *Metallurgy physical chemistry* (Beijing: Metallurgical industry press, 2006),114-126.
9. J. L. Zhang, G W. Wang, and J. G Shao, "A modified random pore model for the kinetics of char gasification," *BioResource*, 9(2) (2014), 3497-3507.
10. J. S. Gupta, and S. K. Bhatia, "A modified discrete random pore model allowing for different initial surface reactivity," *Carbon*, 38(1) (2000), 47-58.
11. C. R. Zhang, Y. G. Yang, and G. Zhang, "Kinetic model for solid state reactions controlled by diffusion," *ACTA physico-chimica sinica*, 4(5) (1988), 539-544.
12. C. J. Ping, J. H. Zhou, and J. Cheng, "Research on the pyrolysis kinetics of blended coals," *Proceedings of the CSEE*, 27(17) (2007), 6-10.
13. Z. X. Fu, Z. C. Guo, and Z. F. Yuan, "Swelling and shrinkage behavior of raw and processed coals during pyrolysis," *Fuel*, 86 (2007), 418– 425.
14. F. Ferrara, A. Orsini, and A. Plaisant, "Pyrolysis of coal, biomass and their blends: Performance assessment by thermogravimetric analysis," *Bioresource Technology*, 171 (2014), 433– 441.
15. M. Ishida, and C. Y. Wen, "Comparison of kinetic and diffusional models for solid-gas reactions," *AIChE J*, 14 (2) (1968), 311-317.